Cortical Circuit Dysfunction in a Mouse Model of Alpha-synucleinopathy in Vivo

Sonja Blumenstock
Max Planck Institute for Neurobiology
Fanfan Sun
German Centre for Neurodegenerative Diseases: Deutsches Zentrum fur Neurodegenerative Erkrankungen
Petar Marinkovic
German Centre for Neurodegenerative Diseases: Deutsches Zentrum fur Neurodegenerative Erkrankungen
Carmelo Sgobio
German Centre for Neurodegenerative Diseases: Deutsches Zentrum fur Neurodegenerative Erkrankungen
Sabine Liebscher (sabine.liebscher@med.uni-muenchen.de)
Klinikum der Universität München, LMU Munich https://orcid.org/0000-0001-5633-8981
Jochen Herms
German Centre for Neurodegenerative Diseases: Deutsches Zentrum fur Neurodegenerative Erkrankungen

Short report

Keywords: Synucleinopathy, templated misfolding, alpha-synuclein, in vivo two-photon calcium imaging, cortex, awake, behaving, Parkinson's disease, Lewy body dementia, seeding

Posted Date: November 24th, 2020

DOI: https://doi.org/10.21203/rs.3.rs-112938/v1

Version of Record: A version of this preprint was published at Brain Communications on January 1st, 2021. See the published version at https://doi.org/10.1093/braincomms/fcab273.

Cortical circuit dysfunction in a mouse model of alpha-synucleinopathy *in vivo*

Running head: Cortical hyperreactivity in alpha-synuclein seeded mice

Sonja Blumenstock, PhD[1,2,3,4,8], Fanfan Sun, MSc[1,8], Petar Marinković, PhD[1,5], Carmelo Sgobio, PhD[1], Sabine Liebscher, MD, PhD[3,6,7]* and Jochen Herms, MD[1,2,3]*

[1]German Center for Neurodegenerative Diseases (DZNE), 81377 Munich, Germany
[2]Center for Neuropathology and Prion Research, Ludwig-Maximilians University Munich, 81377 Munich, Germany
[3]Munich Cluster for Systems Neurology (SyNergy), 81377 Munich, Germany
[4]Current Address: Molecular Neurodegeneration research group, Max Planck Institute of Neurobiology, 82152 Martinsried, Germany
[5]Current Address: Department of Pharmacy, Ludwig-Maximilians University, 81377 Munich, Germany
[6]Institute of Clinical Neuroimmunology, Klinikum der Universität München, Ludwig-Maximilians University, 82152 Martinsried, Germany
[7]Biomedical Center, Medical Faculty, Ludwig-Maximilians University Munich, 82152 Martinsried, Germany

[8] these authors contributed equally

* shared senior authors

Sonja Blumenstock blumenstock@neuro.mpg.de

FanFan Sun fanfan.sun@med.uni-muenchen.de

Petar Marinkovic petar.marinkovic@cup.lmu.de

Carmelo Sgobio csgobio@med.lmu.de

Sabine Liebscher sabine.liebscher@med.uni-muenchen.de

Jochen Herms jochen.herms@med.uni-muenchen.de

Key words

Synucleinopathy, templated misfolding, alpha-synuclein, *in vivo* two-photon calcium imaging, cortex, awake, behaving, Parkinson's disease, Lewy body dementia, seeding

Abstract

Considerable fluctuations in cognitive performance and eventual dementia are an important characteristic of alpha-synucleinopathies, such as Parkinson's disease (PD) and Lewy Body dementia (LBD) and are linked to cortical dysfunction. The presence of misfolded and aggregated alpha-synuclein (a-syn) in the cerebral cortex of patients has been suggested to play a crucial role in this process. However, the consequences of a-syn accumulation on the function of cortical networks at cellular resolution *in vivo* are largely unknown. Here we used the striatal seeding model in wildtype mice in order to induce robust a-synuclein pathology in the cerebral cortex. 9 months after a single intrastriatal injection of a-syn preformed fibrils, we performed in vivo two-photon calcium imaging in awake mice. We observed profound alterations of the function of layer 2/3 cortical neurons in somatosensory cortex (S1), as witnessed by an enhanced response to whisking and increased synchrony, accompanied by a decrease in baseline Ca2+ levels. Stereological analyses revealed a reduction in GAD67-positive inhibitory cells in S1 in PFF-injected brains. These findings point to a disturbed excitation/inhibition balance as an important driver of circuit dysfunction in alpha-synucleinopathies, which may underly cognitive changes in these diseases.

Main text

Parkinson's disease (PD) and other alpha-synucleinopathies are not only characterized by progressive worsening of motor symptoms, but also by cognitive deficits, which can strongly fluctuate over short time scales and which are poorly understood mechanistically to date [1]. In addition to the well-known degeneration within the basal ganglia, there is also ample evidence for a pathophysiological involvement of cortical areas in alpha-synucleinopathies, which has been linked to the cognitive decline [2-4], but actual mechanistic insight is scarce. At the molecular and cellular level, a link between the misfolding, self-aggregation and deposition of the native protein a-synuclein (a-syn) and intraneuronal impairments has been established. Amongst others it has been shown that pathological conformers of a-syn cause various dysfunctions in e.g. ER-to-Golgi trafficking, cytoskeleton dynamics, protein degradation, synaptic vesicle cycle and calcium homeostasis [5, 6]. Importantly, a-syn has also been shown to spread along anatomically connected structures [7], which can be initiated by various molecular forms of a-syn, such as monomers, oligomers or fibrils. When applied acutely in cell culture, preformed recombinant a-syn fibrils (PFFs) can compromise neuronal excitability, trigger intracellular a-syn pathology and cause a rapid loss of spines [8], the latter of which is also observed *in vivo* [9]. However, the underlying relationship between local a-syn aggregation following its templated misfolding and neuronal network dysfunction *in vivo* remains poorly understood. We here thus address the question of how a-syn is affecting cortical circuit function in a mouse model of a-synucleinopathy. To this end we conduct *in vivo* two-photon calcium imaging in somatosensory cortex of awake mice 9 months after a unilateral striatal infusion of PFFs and performed stereological analyses to quantify the number of interneurons in the same area.

Methods

Animals

Wildtype (WT) C57BL/6 mice (Jackson Laboratory) were housed in groups, with food and water provided ad libitum (12/12 hour light/dark cycle). After cranial window implantation, mice were housed separately. All experiments were approved by the Bavarian government (Az. 55.2-1-54-2532-163-13).

PFF purification and seeding

Recombinant WT mouse a-synuclein was purified as described [10, 11]. Preformed fibrils (PFFs) were assembled from purified a-synuclein monomer (5mg/ml) by incubation at 37°C and 1400 rpm for 96hours and stored at -80°C [12]. Directly before injection, PFFs were sonicated (SonoPuls Mini 20). Two month-old mice were anesthetized with ketamine/xylazine (0.13/0.01 mg/g) and stereotactically injected with 5µl (25µg) of PFFs into the dorsal striatum (coordinates relative to the Bregma: +0.2mm anterior, +2.0mm from midline, +2.6mm beneath the dura) of the right hemisphere. Control animals received 5µl sterile PBS.

Virus injection and cranial window implantation

Eight months after PFF-seeding, a cranial window was implanted as reported [9]. In short, mice were anesthetized (ketamine/xylazine) and received dexamethasone (0.01mg/g intraperitoneally) right before surgery. A 4mm in diameter piece of the skull over the right hemisphere (~1mm caudal from bregma, 3mm lateral from midline) was removed, using a dental drill. AAV2/1.hSyn1.mRuby2.GSG.P2A.GCaMP6s.WPRE.SV4 [13] was injected into 3-4 locations within the cranial window (300nl/spot, 0.2mm beneath the dura, virus titer ~10^{12} GC/ml) and the craniotomy sealed with a coverslip using dental acrylic. A headbar was glued next to the coverslip to allow repositioning of the mouse during imaging. After surgery, mice received Carprophen (5 mg/kg, s.c.) and Cefotaxim (0.06mg/kg).

In vivo imaging

Imaging was performed in awake, head-fixed mice [14], 4 weeks after window preparation. Neuronal activity in layer 2/3 of S1 (depth 200–300µm) was probed, using a La Vision Trim Scope (La Vision BioTec GmbH, at 10Hz frame rates, field of view (FOV) of 220x220µm at 223

pixel resolution) equipped with a Ti:sapphire two-photon laser (Mai Tai, Spectra Physics), tuned to 940 nm to simultaneously excite mRuby2 and GCaMP6s and emitted light was split at 560nm and green light (495-560nm, band pass filter) and red light (>560nm) were detected by photomultiplier tubes. Mouse behavior was recorded by a web-camera (pco.pixelfly USB camera) controlled by La Vison Imspector software to synchronize it with the imaging data acquisition. Neuronal activity was also investigated under isoflurane anesthesia (0.5-1 vol%). Body temperature was kept stable with a heating pad, arterial saturation, breathing and heart rate were monitored by pulse oxymeter.

Data processing and analysis

Collected images were analyzed using custom-written codes in MATLAB and ImageJ. Based on whisker movement, mouse behavior was classified as “active” (during whisking) or “quiet”. Two-photon imaging data was registered, to correct for slight brain displacement based on the mRuby2 channel. Regions of interest (ROIs) were manually identified using custom-written software in MATLAB and GCaMP6s fluorescence was constructed by averaging the pixel values within the ROI for each imaging frame. Time-series were corrected for contamination by local neuropil fluorescence [15].

Traces were low pass filtered at 5Hz and slow fluctuations removed by subtracting the 8th percentile within a sliding window of 1000 frames. To estimate F0, we subtracted the 8th percentile in a sliding window of 1 second and used the median of all values below the 70th percentile of this ‘noise band’ as F0. ROIs were classified as active, if $\Delta F/F$ exceeded 3x of the standard deviation of the noise band for at least 10 frames (1 second). Whisking-associated neuronal activity was assessed by considering transients occurring within a window of 1 second before whisking onset up to 2 seconds after whisking offset. All other transients were considered spontaneous activity.

The correlation of neuronal activity for all pairs of active neurons in each field of view was assessed by computing the Pearson correlation coefficient. To this end traces were smoothed over 25 frames and values lower than 2x standard deviation of the noise band were set to 0. The correlation of activity during whisking and stationary epochs was analysed separately and compared to pairwise correlations derived from shuffled data that was generated by circularly shifting each trace at a random value between 1 to the length of the activity trace. In total we recorded from 1561 neurons in 32 experiments (field of views) from 7 control mice and 1534 neurons in 32 experiments from 7 a-syn mice.

Immunohistochemistry

After imaging, mice (control, n=5, a-syn, n=5) were transcardially perfused (4% paraformaldehyde), brains post-fixed in 4% paraformaldehyde overnight and cut into coronal sections (50µm) on a vibratome. Floating sections were stained using anti-Alpha-synuclein-phospho S129 (rabbit polyclonal, Abcam) and anti-GAD67 (mouse monoclonal, Millipore) antibodies, at 1:1000 dilution, for 48h at 4°C. Secondary antibodies (1:1000; goat anti-rabbit Alexa 488, goat anti-mouse Alexa 647, Invitrogen) were incubated overnight at 4℃, followed by an incubation with NeuroTrace 530/615 (1:500, ThermoFisher).

Stereology

Brain sections were scanned on a Zeiss fluorescent microscope (Imager.M2, ZEISS) and analysed using StereoInvestigator® (MBF Bioscience). 7 serial coronal sections spanning the entire hemisphere in the coronal plane, spaced by 600µm were analysed. Outline and fiduciary markers were drawn at 2.5x magnification (EC-Plan-NEOFLUAR 2.5X/0.075, ZEISS) using the Neurotrace stain to delineate reference points. Limits for areas of interest were drawn following the mouse brain Atlas [16]. The investigator was blind to genotype and treatment. Cell analysis was performed at 63x magnification (Plan/APOCHROMAT 63X/1.4 Oil DIC, ZEISS), using a 3D counting frame in a sampling grid (Suppl. Table 1). The coefficient of error (Gundersen), m=1, and the average cell counts per sampling site are described for each marker and region (Suppl. Table 1).

Statistics

We employed student's t-test to compare the average of normally distributed data (e.g. population response to whisking). For non-normally distributed data we used the ranksum (Mann-Whitney-U) test (e.g. fraction of whisking responsive neurons). Distribution of data was compared using the Kolmogorov-Smirnov test (KS, e.g. distribution of frequencies, amplitudes, correlation coefficients). Stereology results were compared using a two-way ANOVA followed by Bonferroni's *post-hoc* test.

Results

Injection of a-syn preformed fibrils induces formation of Lewy-neurite like aggregates in cortex of WT mice

The injection of a-syn PFFs into the dorsal striatum triggers the formation of intracellular Lewy-neurite like aggregates in remotely connected areas in the brain. Intracellular phosphorylated a-syn aggregates are found across all layers in somatosensory cortex 9 months after the injection of PFFs, with the highest density in infragranular layers, which contain extensive projections to the dorsal striatum (Suppl. Fig. S1).

Hyperreactivity in somatosensory cortex in a-syn PFF injected mice

In vivo two-photon calcium imaging in awake mice was conducted 9 months after PFF-seeding (Fig. 1A-C). We observed a pronounced increase in responsiveness to individual whisking events both at the population level, as well as on the level of individual neurons (Fig. 1D-F). The average response of active neurons to individual onsets of whisking was significantly increased in a-syn mice (Fig. 1E, area under the curve 0.5–3 seconds after whisking onset (grey area); $P<10^{-19}$, student's t-test). Furthermore, the fraction of neurons responsive to whisking (i.e. neurons that display a significant increase in $\Delta F/F$ within 0.5-1.5 seconds after whisking onset compared to their activity within 0.5 seconds prior to whisking onset) was also significantly increased in a-syn mice (Fig. 1F). We observed a right shift in the distribution of transient frequencies and amplitudes during quiescence (Suppl Fig. S2A,B) and during whisking-epochs (Suppl Fig. S2A,B) in a-syn compared to control mice. The overall time spend whisking did not differ between control and a-syn mice (P=0.45, ranksum test). The level of spontaneous activity correlated well with the whisking-associated activity levels in both control and a-syn mice (Fig. 1G). To characterize and quantify the relationship between spontaneous versus whisking-associated neuronal activity for each cell, we computed the angle of each data point in a plot displaying the whisking-associated versus spontaneous frequency (Fig. 1G). This analysis revealed that the distribution of angles was significantly different in a-syn mice (Fig. 1H), with a larger fraction of neurons favoring activity during whisking over spontaneous activity. Neuronal activity did also not differ between control and a-syn mice during anesthesia (Suppl. Fig 2C,D). In addition, we addressed the question whether baseline calcium levels might also be affected in a-syn PFF-seeded mice. To this end, we took advantage of the stoichiometric expression of

both fluorophores mRuby2 and GCaMP6s. We computed the ratio between baseline values of the green and red channel (G/R ratio). On average neurons in a-syn PFF-seeded mice had a slightly, yet significantly, lower ratio compared to control mice (Suppl. Fig. S2G), indicating that the baseline calcium content is lower in neurons in a-syn PFF-seeded mice. Pairwise neuronal correlations during stationary epochs were not affected (Fig. 2A-C), while whisking-associated neuronal activity appeared more correlated (Fig. 2D) upon PFF seeding.

Stereological analysis of GABAergic interneurons

We found a reduction in the number of GAD67-positive inhibitory cells (Fig. 3A-C), which was most prominently seen for layer 5/6. This reduction was specific to inhibitory neurons as the overall number of neurons was not affected (Fig. 3D) and also the cortical volume was not changed (Fig. 3E) by the injection of PFFs.

Discussion

Cortical dysfunction is central to the development of the cognitive decline in a-synucleinopathies, such as PD and LBD [2-4]. However, the consequences of pathological a-syn on neuronal network function, particularly in the cerebral cortex, remain poorly understood. To address this question, we recorded neuronal activity in awake, behaving mice using two-photon calcium imaging 9 months after a single intrastriatal injection of a-syn PFFs. Striatal seeding of PFFs caused neuritic and somatic inclusions across all cortical layers, accompanied by a loss of dendritic spines in S1, a region upstream of the inoculated striatum [9]. We here now demonstrate that the striatal seeding model is also causing cortical neuronal dysfunction. Our *in vivo* imaging approach revealed a pronounced increase in neuronal activity in response to whisking (hyperreactivity) in a-syn PFF-injected mice. The observed elevated population response in S1 can be attributed to an increase in the fraction of whisking responsive cells and suggests an altered excitation/inhibition balance. Furthermore, stronger pairwise neuronal activity correlations indicate increased network synchrony. Acute application of PFFs has recently been shown to cause spine loss reduce and neuronal activity [8]. Our data, however, suggest that under chronic conditions *in vivo,* PFF-seeding can cause the opposite effect on the network level. Mechanistically, we could attribute the observed hyperreactivity to a loss of ~25% of GAD67-positive interneurons in S1 in a-syn PFF-seeded mice, occurring after the long incubation period of 9 months. This pronounced drop in overall GABAergic neuron number is likely causing an inhibitory deficit within the local microcircuitry. Earlier studies reported increased excitatory transmission, disturbed calcium homeostasis with elevated intracellular baseline Ca^{2+} levels due to oligomer-mediated pore formation in the postsynaptic membrane, enhanced voltage-operated Ca^{2+} channel activity or inefficient membrane repolarization in response to pathological a-syn [5, 17-19]. However, most of these reports are based on cell culture or artificial phospholipid membranes and rely on overexpression or acute application of high concentrations of a-syn. In the *in vivo* scenario, we here observed a reduction of baseline Ca^{2+} levels in awake mice. Interestingly, a recent publication is showing reduced cytosolic Ca^{2+} concentration at early stages of the degenerative process in cultured cells, while only at later stages Ca^{2+} levels increased [20]. It is important to remember that in both our seeded mice and in humans, the majority of cortical neurons are actually free of Lewy-neurite like aggregates and therefore are likely exposed to disease-mechanisms other than an overload of fibrillar a-syn. The prolonged state of progressive a-syn aggregation in a subset of neurons in our model more closely reflects the mostly sporadic human pathophysiology than transgenic mice

overexpressing a-syn or cultured cells and tissues do. Importantly, hyperactivation of sensorimotor cortical areas was also shown in electrophysiological and functional magnetic resonance imaging studies conducted in parkinsonian rats and patients and have been attributed to both motor and psychotic symptoms in synucleinopathies [21-23]. These data strongly emphasize the translational relevance of our findings also for human pathophysiology. Dysregulation of cortical activity in turn could lead to profound changes in the downstream striatum. Functional studies at cellular resolution are therefore crucial for defining the exact relationships in parkinsonian networks.

Conclusion

We here provide compelling evidence for a functional impact of seeded a-syn on cortical networks by overall increasing excitability, likely through the selective vulnerability of interneurons. Our data also demonstrate that chronic effects of a-syn accumulation can strongly differ from acute effects, causing an opposite impact at the network level through cell-type specific vulnerability, supporting the notion that spreading of a-syn alters the excitatory/inhibitory balance in cortical circuits.

List of abbrevations

a-syn – alpha-synuclein

Ca^{2+} – calcium ions

ER – endoplasmic reticulum

FOV – field of view

GABA - gamma-aminobutyric acid

GAD67 – glutamic acid decarboxylase 67

KS – Kolmogorov-Smirnov

LBD – Lewy body dementia

PD – Parkinson’s disease

ROI – region of interest

WT - wildtype

PFF – preformed fibrils

S1 – primary somatosensory cortex

Declarations

Ethics approval

All experiments were approved by the Bavarian government (Az. 55.2-1-54-2532-163-13).

Consent for publication

Not applicable

Availability of data and material

The datasets used and/or analysed during the current study available from the corresponding author on reasonable request.

Competing interests

The authors declare that they have no competing interests.

Author Contributions

Conception and design of study (SB, JH), data acquisition (SB, FS), setup design / data acquisition assistance (PM) software development (SL), data analysis (SB, FS, CS, SL), data interpretation (SB, CB, SL, JH), manuscript preparation (SB, SL, help from all authors), securing funding (JH) and project supervision (SL, JH).

Acknowledgements

We are particularly grateful to Pieter Goltstein for developing and sharing software for data analysis. We also thank Eric Grießinger, Sarah Hanselka, and Nadine Lachner for excellent

technical support. We are grateful to the Genetically-Encoded Neuronal Indicator and Effector (GENIE) Project and the Janelia Farm Research Campus of the Howard Hughes Medical Institute, in particular to Vivek Jayaraman, Rex A. Kerr, Douglas S. Kim, Loren L. Looger, and Karel Svoboda for developing and distributing the genetically encoded calcium indicator GCaMP6s.

Funding

This work was funded by the Deutsche Forschungsgemeinschaft (DFG, German Research Foundation) under Germany's Excellence Strategy within the framework of the Munich Cluster for Systems Neurology - EXC 2145 SyNergy – ID 390857198 (SL, JH), EXC 1010 (SB), the DFG, Emmy Noether Programme (SL).

References

1. Matar E, Shine JM, Halliday GM, Lewis SJG: **Cognitive fluctuations in Lewy body dementia: towards a pathophysiological framework.** *Brain* 2020, **143:**31-46.
2. Colloby SJ, Watson R, Blamire AM, O'Brien JT, Taylor JP: **Cortical thinning in dementia with Lewy bodies and Parkinson disease dementia.** *Aust N Z J Psychiatry* 2020, **54:**633-643.
3. Caviness JN, Lue LF, Hentz JG, Schmitz CT, Adler CH, Shill HA, Sabbagh MN, Beach TG, Walker DG: **Cortical phosphorylated alpha-Synuclein levels correlate with brain wave spectra in Parkinson's disease.** *Mov Disord* 2016, **31:**1012-1019.
4. Hurtig HI, Trojanowski JQ, Galvin J, Ewbank D, Schmidt ML, Lee VM, Clark CM, Glosser G, Stern MB, Gollomp SM, Arnold SE: **Alpha-synuclein cortical Lewy bodies correlate with dementia in Parkinson's disease.** *Neurology* 2000, **54:**1916-1921.
5. Reznichenko L, Cheng Q, Nizar K, Gratiy SL, Saisan PA, Rockenstein EM, González T, Patrick C, Spencer B, Desplats P, et al: **In Vivo Alterations in Calcium Buffering Capacity in Transgenic Mouse Model of Synucleinopathy.** *The Journal of Neuroscience* 2012, **32:**9992–9998.
6. Wong YC, Krainc D: **α-synuclein toxicity in neurodegeneration: mechanism and therapeutic strategies.** *Nature Medicine* 2017, **23:**1–13.
7. Uchihara T, Giasson BI: **Propagation of alpha-synuclein pathology: hypotheses, discoveries, and yet unresolved questions from experimental and human brain studies.** *Acta Neuropathologica* 2016, **131:**49–73.
8. Wu Q, Takano H, Riddle DM, Trojanowski JQ, Coulter DA, Lee VM: **alpha-Synuclein (alphaSyn) Preformed Fibrils Induce Endogenous alphaSyn Aggregation, Compromise Synaptic Activity and Enhance Synapse Loss in Cultured Excitatory Hippocampal Neurons.** *J Neurosci* 2019, **39:**5080-5094.
9. Blumenstock S, Rodrigues EF, Peters F, Blazquez-Llorca L, Schmidt F, Giese A, Herms J: **Seeding and transgenic overexpression of alpha-synuclein triggers dendritic spine pathology in the neocortex.** *EMBO Molecular Medicine* 2017, **9:**716–731.
10. Nuscher B, Kamp F, Mehnert T, Odoy S, Haass C, Kahle PJ, Beyer K: **α-Synuclein Has a High Affinity for Packing Defects in a Bilayer Membrane A THERMODYNAMICS STUDY.** *Journal of Biological Chemistry* 2004, **279:**21966–21975.
11. Kostka M, Högen T, Danzer KM, Levin J, Habeck M, Wirth A, Wagner R, Glabe CG, Finger S, Heinzelmann U, et al: **Single Particle Characterization of Iron-induced Pore-forming α-Synuclein Oligomers.** *Journal of Biological Chemistry* 2008, **283:**10992–11003.
12. Conway KA, Harper JD, Lansbury PT: **Fibrils Formed in Vitro from α-Synuclein and Two Mutant Forms Linked to Parkinson's Disease are Typical Amyloid \textsuperscript†.** *Biochemistry* 2000, **39:**2552–2563.
13. Rose T, Jaepel J, Hübener M, Bonhoeffer T: **Cell-specific restoration of stimulus preference after monocular deprivation in the visual cortex.** *Science (New York, NY)* 2016, **352:**1319–1322.
14. Guo ZV, Hires SA, Li N, O'Connor DH, Komiyama T, Ophir E, Huber D, Bonardi C, Morandell K, Gutnisky D, et al: **Procedures for behavioral experiments in head-fixed mice.** *PloS One* 2014, **9:**e88678.
15. Liebscher S, Keller GB, Goltstein PM, Bonhoeffer T, Hübener M: **Selective Persistence of Sensorimotor Mismatch Signals in Visual Cortex of Behaving Alzheimer's Disease Mice.** *Current Biology* 2016, **26:**956–964.

16. Paxinos G, Franklin KB: *Paxinos and Franklin's the Mouse Brain in Stereotaxic Coordinates, Compact - 5th Edition.* 2013.
17. Schmidt F, Levin J, Kamp F, Kretzschmar H, Giese A, Bötzel K: **Single-Channel Electrophysiology Reveals a Distinct and Uniform Pore Complex Formed by α-Synuclein Oligomers in Lipid Membranes.** *PLoS ONE* 2012, **7:**e42545.
18. Hettiarachchi NT, Parker A, Dallas ML, Pennington K, Hung C-C, Pearson HA, Boyle JP, Robinson P, Peers C: **α-Synuclein modulation of Ca2+ signaling in human neuroblastoma (SH-SY5Y) cells.** *Journal of Neurochemistry* 2009, **111:**1192–1201.
19. Shrivastava AN, Redeker V, Fritz N, Pieri L, Almeida LG, Spolidoro M, Liebmann T, Bousset L, Renner M, Lena C, et al: **α-synuclein assemblies sequester neuronal 3-Na+/K+-ATPase and impair Na+ gradient.** *The EMBO Journal* 2015, **34:**2408–2423.
20. Betzer C, Lassen LB, Olsen A, Kofoed RH, Reimer L, Gregersen E, Zheng J, Calì T, Gai WP, Chen T, et al: **Alpha-synuclein aggregates activate calcium pump SERCA leading to calcium dysregulation.** *EMBO reports* 2018, **19:**e44617.
21. Li Q, Ke Y, Chan DCW, Qian Z-M, Yung KKL, Ko H, Arbuthnott GW, Yung W-H: **Therapeutic Deep Brain Stimulation in Parkinsonian Rats Directly Influences Motor Cortex.** *Neuron* 2012, **76:**1030–1041.
22. Yu H, Sternad D, Corcos DM, Vaillancourt DE: **Role of hyperactive cerebellum and motor cortex in Parkinson's disease.** *NeuroImage* 2007, **35:**222–233.
23. Nagahama Y, Okina T, Suzuki N, Matsuda M: **Neural correlates of psychotic symptoms in dementia with Lewy bodies.** *Brain* 2010, **133:**557–567.

Figure Legends

Figure 1. Neuronal hyperreactivity in S1 upon striatal injection of a-syn PFFs.

(A) Timeline of experiments. Mice received a striatal injection of PFFs at the age of 2 months, followed by the injection of AAV2/1.hSyn1.mRuby2.P2A.GCaMP6s into the somatosensory cortex (S1) and the implantation of a cranial window 8 months later when PFFs are globally present (assessed by immunofluorescence of phospho- synuclein (pSYN)). One month later *in vivo* imaging experiments were performed, after which mice were sacrificed and stereology was conducted. **(B)** Representative example of a field of view (FOV). **(C)** Calcium traces of individual regions of interest (ROIs) are shown for control and a-syn mice and referenced by whisking activity (gray lines). **(D)** Heat maps depicting the average neural response to whisking onset (white line, normalized to the average activity within 1 sec before whisking onset) for whisking responsive cells (control: 187 of 1561 neurons, a-syn: 276 of 1534 neurons). **(E)** Population response of active neurons to whisking onset. **(F)** Fraction of whisking responsive neurons in each experiment (P=0.003, ranksum test, control n=32 experiments, a-syn n=32 experiments). **(G)** Relationship of the stationary neuronal frequency and the activity associated with whisking in control (black) and a-syn mice (red, control R^2=0.63, y=1.36x–0.07; P<0.0001; a-syn R^2=0.63, y=1.26x+0.44, P<0.0001). To compare state-specific neuronal activity levels, the angle α was computed for each neuron, as exemplified for one neuron (light blue line and angle). **(H)** The distribution of all angles is significantly different in a-syn mice, with more neurons favoring activity during whisking epochs (angle of 0° indicates neuronal activity exclusively during stationary (quiescent) epochs, while 90° would indicate exclusive whisking-associated neuronal activity, $P<10^{-4}$, KS test). Data are mean +/- SEM. Scale bar in B is 50µm. ** P < 0.01, *** P < 0.001

Figure 2. Striatal PFF seeding elevates pairwise neuronal correlations during whisking in S1

(A) Example raster plot depicting activity of each ROI within an FOV referenced by whisking (purple area). **(B)** Correlograms of pairwise correlations during stationary and whisking-associated epochs in a control and an a-syn mouse. **(C)** Average pairwise correlations of individual experiments did not differ (P=0.43, KS test), while **(D)** whisking-associated correlations were significantly increased in a-syn compared to control mice and each to shuffled data (control vs a-syn P=0.026, control vs shuffled control P<0.0001, a-syn vs shuffled a-syn P<0.0001, KS test). Data are individual experiments superimposed by the median +/- 95% confidence interval (C,D). * P < 0.05, *** P < 0.0001.

Figure 3. Stereology of somatosensory cortex reveals reduction of inhibitory neurons

(A) Representative examples of immunohistochemical stainings for neurotrace (NT), phospho-synuclein (a-syn, red) and GAD67 (white arrow heads mark GAD67 positive GABAergic neurons) in S1 of a control and an a-syn PFF-seeded mouse assessed 10 months after striatal seeding. **(B)** Brain sections used for stereology to assess overall number of neurons and of GABAergic cells across all cortical layers in the entire S1 area (orange area). **(C)** The number of GAD67 positive neurons was significantly reduced in a-syn mice (two-way ANOVA, effect of group $F(1,32)=14.69$, $P=0.0006$; effect of layer $F(3,32)=35.12$, $P<0.0001$; layer 5/6 $P=0.019$; Bonferroni *post-hoc* test, all other layers n.s), while neither **(D)** the total number of all neurons (effect of group $F(1,32)=1.41$, $P=0.24$, effect of layer $F(3,32)=132.2$, $P<0.0001$), nor **(E)** the cortical volume of S1 was affected (effect of group $F(1,32)=0.78$, $P=0.39$, effect of layer $F(3,32)=530.3$, $P<0.0001$). Data are mean +/- SEM in (C,D,E). Scale bar 100µm in (A). *** $P < 0.0001$.

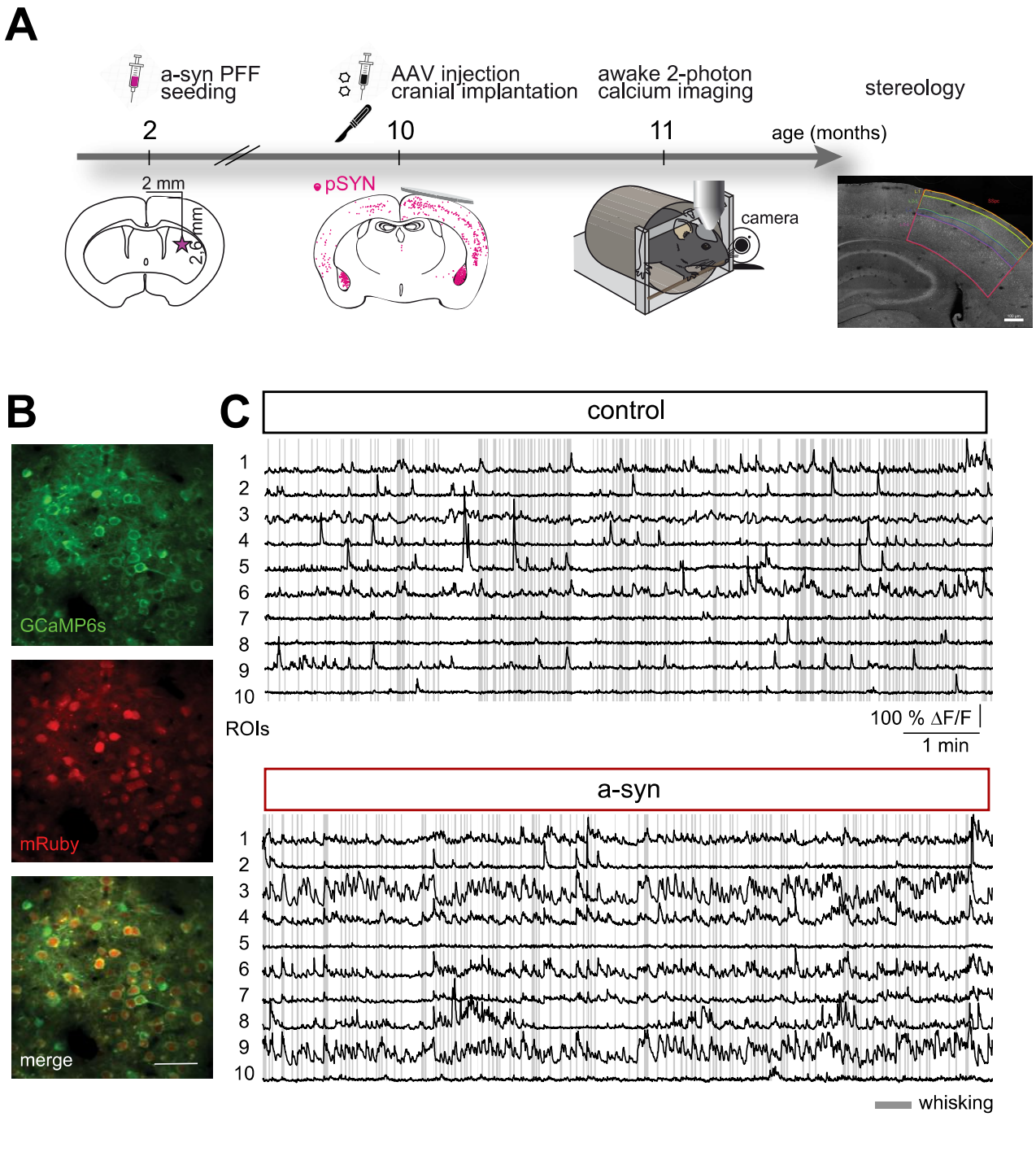
A
a-syn PFF seeding
AAV injection cranial implantation
awake 2-photon calcium imaging
stereology
2
10
11
age (months)
2 mm
2.6 mm
pSYN
camera
B
GCaMP6s
mRuby
merge
C
control
a-syn
ROIs
100 % ΔF/F
1 min
whisking
D
control
a-syn
ROIs
time [sec]
ΔF/F [%]
E
population response whisking (ΔF/F [%])
control
a-syn
***
time [sec]
F
fraction whisking responsive cells
**
control
a-syn
G
control
a-syn
frequency during whisking [trans/min]
frequency stationary [trans/min]
α
H
exclus. whisk. active
angle (α)
fraction cells
***
exclus. spont. active

Figure 1

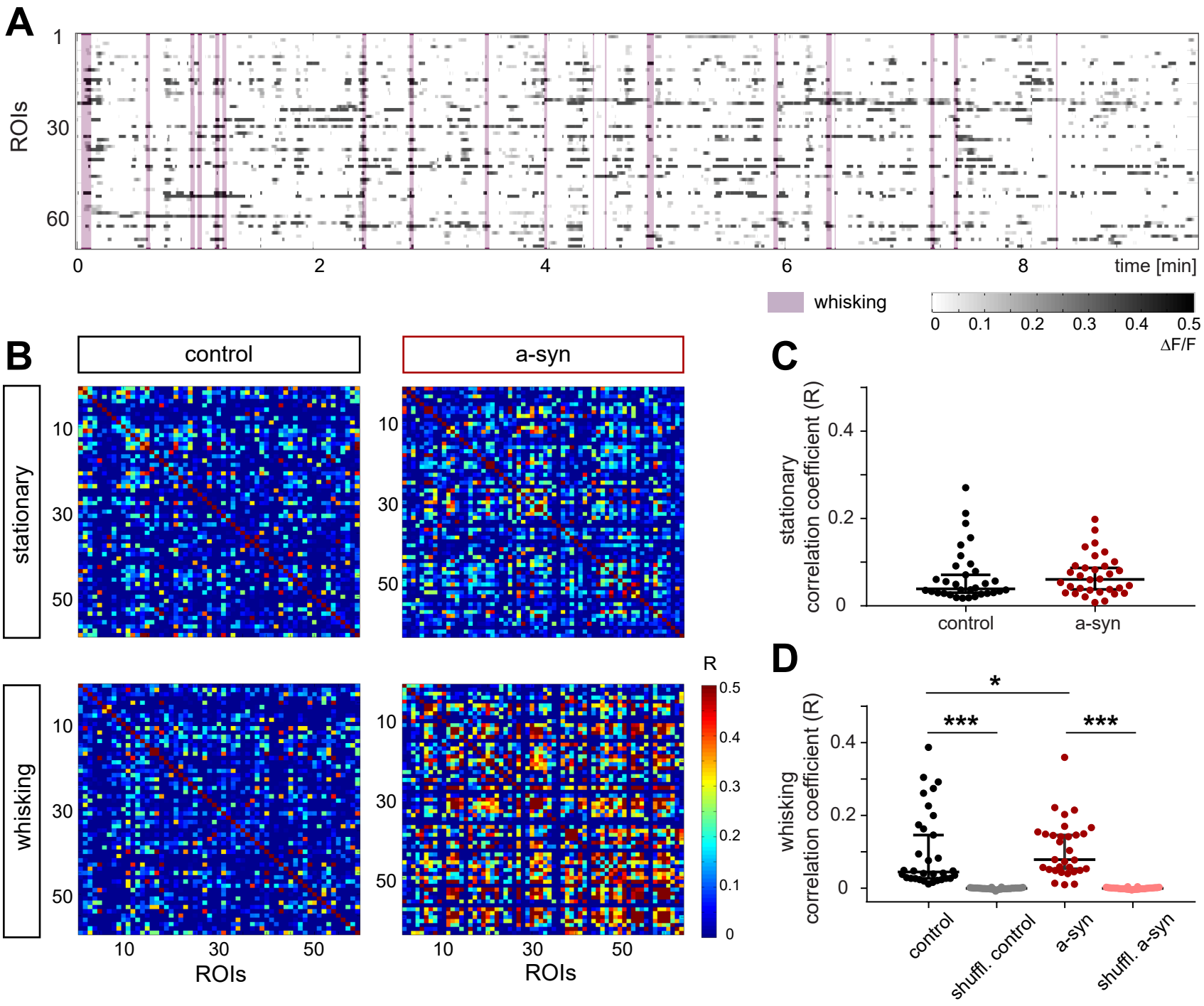
A
ROIs
1
30
60
0
2
4
6
8
time [min]
whisking
0
0.1
0.2
0.3
0.4
0.5
ΔF/F
B
control
a-syn
stationary
whisking
10
30
50
ROIs
R
0.5
0.4
0.3
0.2
0.1
0
C
stationary correlation coefficient (R)
0.4
0.2
0
control
a-syn
D
whisking correlation coefficient (R)
*
***
***
0.4
0.2
0
control
shuffl. control
a-syn
shuffl. a-syn

Figure 2

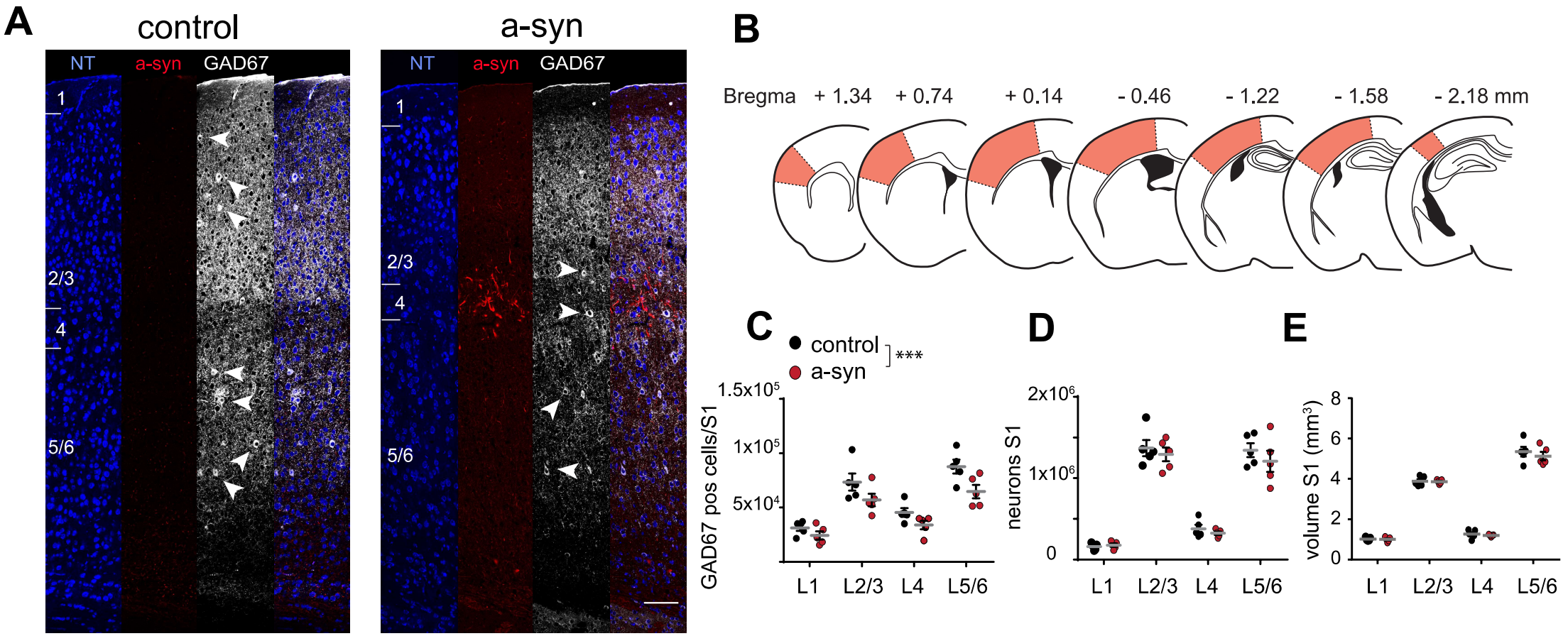
A
control
a-syn
NT
a-syn
GAD67
1
2/3
4
5/6
B
Bregma + 1.34 + 0.74 + 0.14 - 0.46 - 1.22 - 1.58 - 2.18 mm
C
control
a-syn
***
GAD67 pos cells/S1
1.5x10^5
1x10^5
5x10^4
L1 L2/3 L4 L5/6
D
neurons S1
2x10^6
1x10^6
0
L1 L2/3 L4 L5/6
E
volume S1 (mm^3)
8
6
4
2
0
L1 L2/3 L4 L5/6

Figure 3

Figures

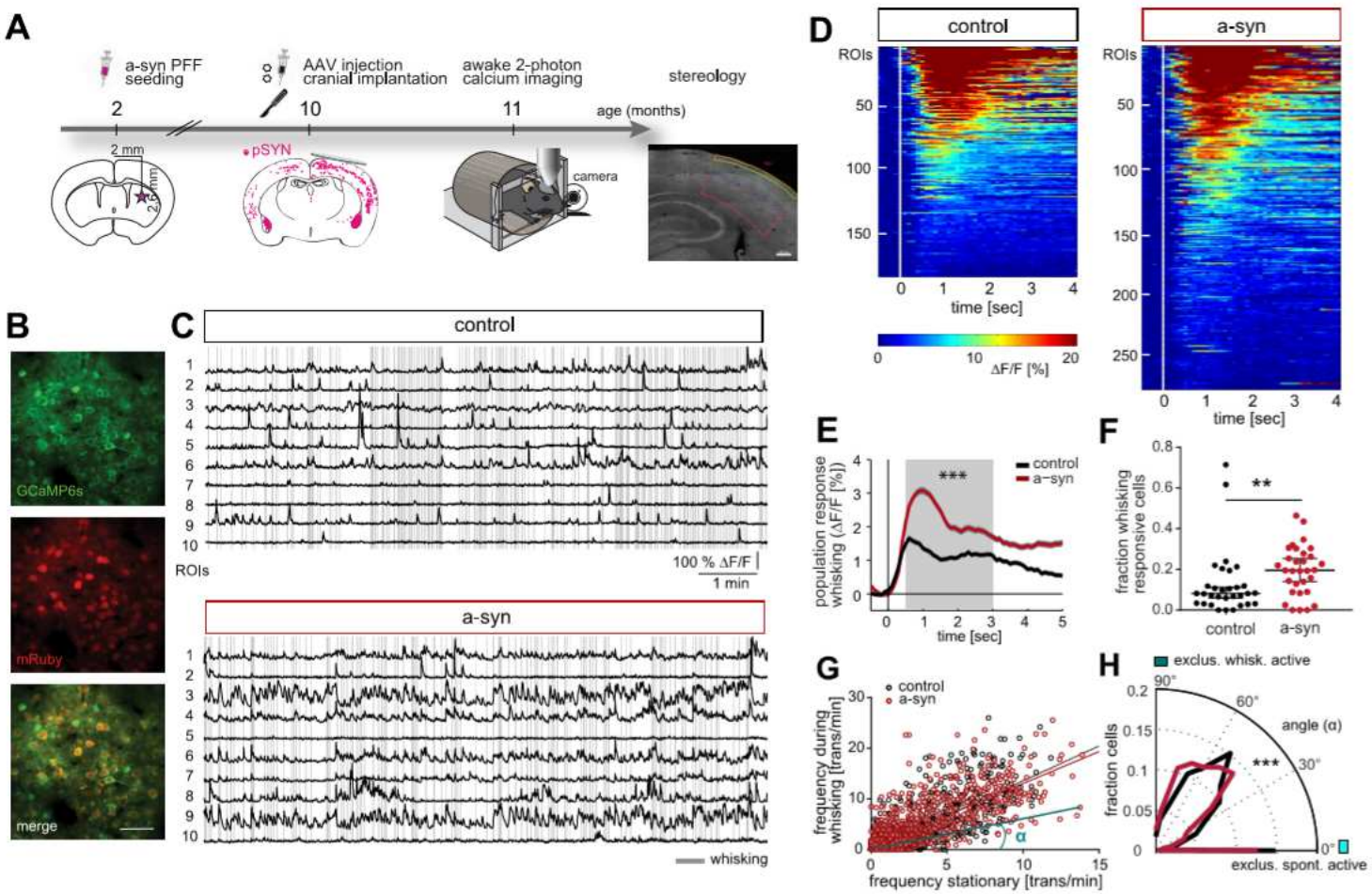

Figure 1

Neuronal hyperreactivity in S1 upon striatal injection of a-syn PFFs. (A) Timeline of experiments. Mice received a striatal injection of PFFs at the age of 2 months, followed by the injection of AAV2/1.hSyn1.mRuby2.P2A.GCaMP6s into the somatosensory cortex (S1) and the implantation of a cranial window 8 months later when PFFs are globally present (assessed by immunofluorescence of phospho- synuclein (pSYN)). One month later in vivo imaging experiments were performed, after which mice were sacrificed and stereology was conducted. (B) Representative example of a field of view (FOV). (C) Calcium traces of individual regions of interest (ROIs) are shown for control and a-syn mice and referenced by whisking activity (gray lines). (D) Heat maps depicting the average neural response to whisking onset (white line, normalized to the average activity within 1 sec before whisking onset) for whisking responsive cells (control: 187 of 1561 neurons, a-syn: 276 of 1534 neurons). (E) Population response of active neurons to whisking onset. (F) Fraction of whisking responsive neurons in each experiment (P=0.003, ranksum test, control n=32 experiments, a-syn n=32 experiments). (G) Relationship of the stationary neuronal frequency and the activity associated with whisking in control (black) and a-syn mice (red, control R2=0.63, y=1.36x−0.07; P<0.0001; a-syn R2=0.63, y=1.26x+0.44, P<0.0001). To compare state-specific neuronal activity levels, the angle α was computed for each neuron, as exemplified

for one neuron (light blue line and angle). (H) The distribution of all angles is significantly different in a-syn mice, with more neurons favoring activity during whisking epochs (angle of 0° indicates neuronal activity exclusively during stationary (quiescent) epochs, while 90° would indicate exclusive whisking-associated neuronal activity, P<10-4, KS test). Data are mean +/- SEM. Scale bar in B is 50µm. ** P < 0.01, *** P < 0.001

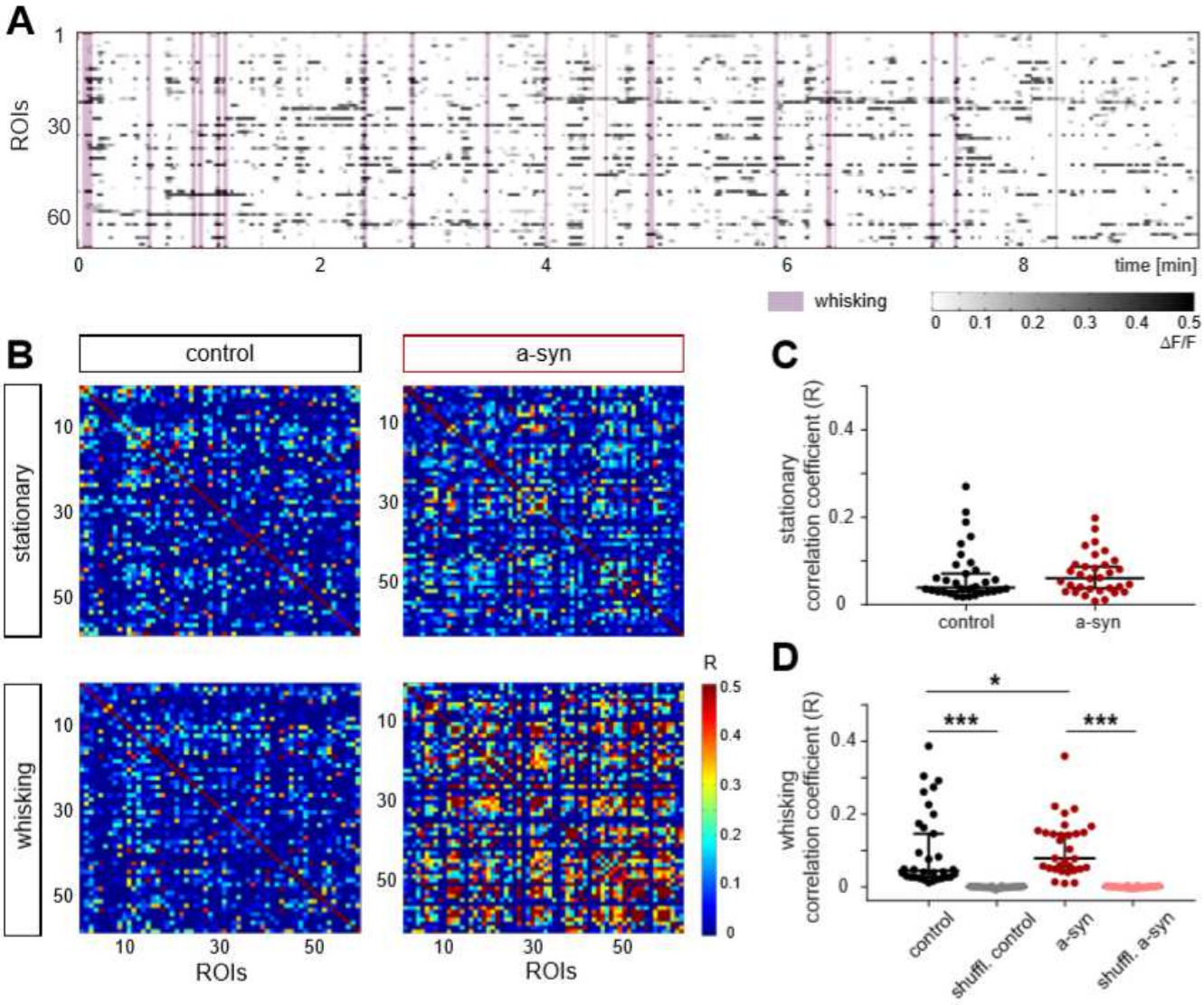

Figure 2

Striatal PFF seeding elevates pairwise neuronal correlations during whisking in S1 (A) Example raster plot depicting activity of each ROI within an FOV referenced by whisking (purple area). (B) Correlograms of pairwise correlations during stationary and whisking-associated epochs in a control and an a-syn mouse. (C) Average pairwise correlations of individual experiments did not differ (P=0.43, KS test), while (D) whisking-associated correlations were significantly increased in a-syn compared to control mice and each to shuffled data (control vs a-syn P=0.026, control vs shuffled control P<0.0001, a-syn vs shuffled a-syn P<0.0001, KS test). Data are individual experiments superimposed by the median +/- 95% confidence interval (C,D). * P < 0.05, *** P < 0.0001.

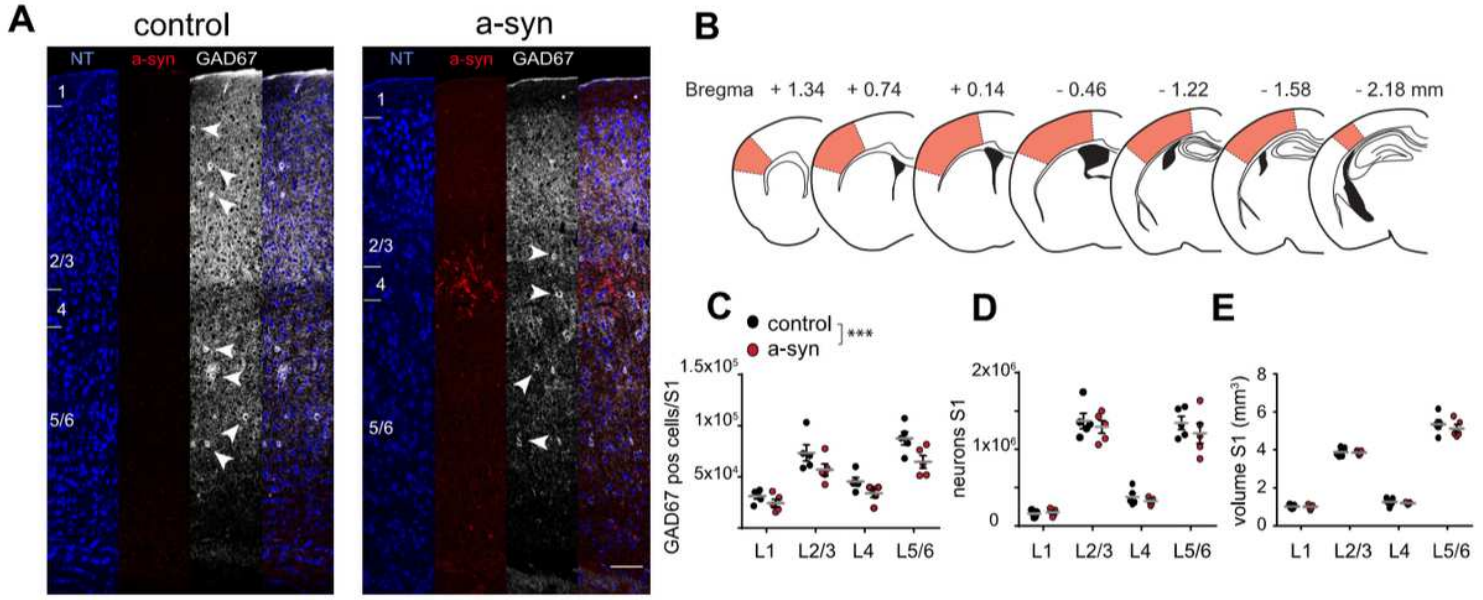

Figure 3

Stereology of somatosensory cortex reveals reduction of inhibitory neurons (A) Representative examples of immunohistochemical stainings for neurotrace (NT), phospho-synuclein (a-syn, red) and GAD67 (white arrow heads mark GAD67 positive GABAergic neurons) in S1 of a control and an a-syn PFF-seeded mouse assessed 10 months after striatal seeding. (B) Brain sections used for stereology to assess overall number of neurons and of GABAergic cells across all cortical layers in the entire S1 area (orange area). (C) The number of GAD67 positive neurons was significantly reduced in asyn mice (two-way ANOVA, effect of group $F(1,32)=14.69$, $P=0.0006$; effect of layer $F(3,32)=35.12$, $P<0.0001$; layer 5/6 $P=0.019$; Bonferroni post-hoc test, all other layers n.s), while neither (D) the total number of all neurons (effect of group $F(1,32)=1.41$, $P=0.24$, effect of layer $F(3,32)=132.2$, $P<0.0001$), nor (E) the cortical volume of S1 was affected (effect of group $F(1,32)=0.78$, $P=0.39$, effect of layer $F(3,32)=530.3$, $P<0.0001$). Data are mean +/- SEM in (C,D,E). Scale bar 100µm in (A). *** $P < 0.0001$.

Supplementary Files

This is a list of supplementary files associated with this preprint. Click to download.

- Blumenstocketalsuppl.pdf